

Photoisomerization of 2-(2-pyrrol-2-ylethenyl)benzoxazole and 2-(2-pyrrol-2-ylethenyl)benzothiazole

2 PERKIN

Masashi Ikegami and Tatsuo Arai*

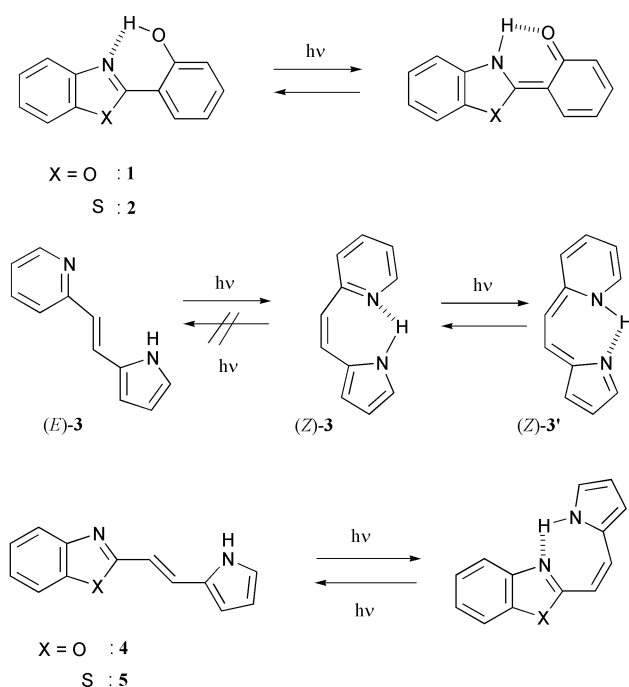
Department of Chemistry, University of Tsukuba, Tsukuba, Ibaraki, 305-8571, Japan.
E-mail: arai@chem.tsukuba.ac.jp; Fax: +81-298-53-6503; Tel: +81-298-53-4521

Received (in Cambridge, UK) 3rd July 2001, Accepted 28th November 2001
First published as an Advance Article on the web 4th January 2002

Hydrogen bonded compounds 2-(2-pyrrol-2-ylethenyl)benzoxazole (**4**) and 2-(2-pyrrol-2-ylethenyl)benzothiazole (**5**) were synthesized and their photochemical behavior was studied. The (*Z*) isomers of **4** and **5** form intramolecular hydrogen bonds as revealed by the ^1H NMR studies. The *trans* isomers are pale yellow in solution, but on photoirradiation, the color changes slightly to a different yellow due to the change of the absorption spectra. The quantum yield of isomerization of **4** and **5** is quite high in the range 0.4–0.6 and is somewhat dependent on the solvent properties. On triplet sensitization **4** and **5** gave T–T absorption spectra with a lifetime of *ca.* 1 μs in benzene. Since a transient absorption spectrum was not observed on direct irradiation of **4** and **5** with a 308 nm laser pulse, the *cis*–*trans* isomerization on direct irradiation should take place in the excited singlet state. On triplet sensitization **4** and **5** underwent *cis*–*trans* isomerization. These results indicate that the intramolecular hydrogen bonding is broken in the singlet excited state as well as in the triplet excited state of (*Z*)-**4** and (*Z*)-**5**.

Introduction

In recent years, intramolecular hydrogen atom transfer in 2-(2-hydroxyphenyl)benzoxazole (**1**) and -benzothiazole (**2**) (Scheme 1) has been extensively investigated by many



Scheme 1

researchers.^{1–8} These molecules underwent intramolecular hydrogen atom transfer to give the tautomer in the excited state exhibiting fluorescence spectra with large Stokes shifts. In addition, transient absorption spectra of the tautomer produced by intramolecular hydrogen atom transfer in the singlet excited state have been observed upon laser flash photolysis in non-polar solvents.

As to the photoisomerization behavior of hydrogen bonded compounds,^{9–15} we have already reported that an olefin with a pyrrole ring and a pyridine ring (**3**) exhibits one-way *trans*–*cis* isomerization due to the presence of intramolecular hydrogen bonding.¹² Furthermore, intramolecular hydrogen atom transfer occurred in the singlet excited state of (*Z*)-**3** to give the tautomer (*Z*)-**3'** upon photoirradiation, which was revealed by the observation of a fluorescence spectrum with a large Stokes shift.¹² In addition, transient absorption spectra due to the tautomer in the ground state were observed upon laser flash photolysis.^{12,13} Therefore, it was of interest to study the photochemical behavior of compounds having isomerizable double bonds in addition to the hydrogen bonding in **1** and **2**.

We wish to report here the preparation of olefins with a pyrrole ring and a benzoxazole ring (**4**) or a benzothiazole ring (**5**) and studies of their photoisomerization behavior. The olefins **4** and **5** are able to undergo *cis*–*trans* isomerization as well as intramolecular hydrogen atom transfer and each reaction was expected to control the efficiency and/or the selectivity of the other reaction processes.

Experimental

Materials and solvents

(*E*)-2-(2-Pyrrol-2-ylethenyl)benzoxazole ((*E*)-**4**) and -benzothiazole ((*E*)-**5**) were prepared by Wittig reaction.¹⁶ *cis*-Isomers were obtained by isomerization of (*E*)-isomers on irradiation at 366 nm. Both *trans*- and *cis*-isomers were purified by column chromatography on silica gel and recrystallized from benzene and hexane, respectively.

(*E*)-2-(2-Pyrrol-2-ylethenyl)benzoxazole ((*E*)-**4**). ^1H NMR (CDCl_3 , 200 MHz) δ (ppm) 6.60 (d, 1H, $J = 16.2$ Hz, olefinic proton), 7.64 (d, 1H, $J = 16.2$ Hz, olefinic proton), 6.32 (m, 1H, pyrrole proton), 6.60 (m, 1H, pyrrole proton), 6.95 (m, 1H, pyrrole proton), 7.30 (m, 1H, benzoxazole proton), 7.50 (m, 1H, benzoxazole proton), 7.64 (m, 1H, benzoxazole proton), 8.6 (NH proton); mp = 213–214 °C. Anal Calcd. for $\text{C}_{13}\text{H}_{10}\text{N}_2\text{O}$:

C, 74.27; H, 4.79; N, 13.33%. Found: C, 74.00; H, 4.84; N, 13.19%.

(Z)-2-(2-Pyrrol-2-ylethenyl)benzoxazole ((Z)-4). ^1H NMR (CDCl_3 , 200 MHz) δ (ppm) 6.09 (d, $J = 13.0$ Hz, 1H, olefinic proton), 6.36 (m, 1H, pyrrole H), 6.57 (m, 1H, pyrrole H), 6.83 (d, 1H, $J = 12.8$ Hz, olefinic proton), 7.17 (m, 1H, pyrrole H), 7.35 (m, 2H, benzoxazole H), 7.49 (m, 1H, benzoxazole H), 7.73 (m, 1H, benzoxazole H), 14.0 (NH proton); mp = 75–76 °C.

(E)-2-(2-Pyrrol-2-ylethenyl)benzothiazole ((E)-5). ^1H NMR (CDCl_3 , 200 MHz) δ (ppm) 6.30 (m, 1H, pyrrole proton), 6.58 (m, 1H, pyrrole proton), 6.94 (d, 1H, $J = 16.2$ Hz, olefinic proton), 6.95 (m, 1H, pyrrole proton), 7.38 (m, 2H, benzothiazole proton), 7.40 (d, 1H, $J = 16.2$ Hz, olefinic proton), 7.83 (dd, 1H, $J = 7.5, 1.2$ Hz, benzothiazole proton), 7.92 (dd, 1H, $J = 7.5, 1.2$, benzothiazole proton), 9.1 (br s, NH proton); mp = 198–199 °C. Anal Calcd. for $\text{C}_{13}\text{H}_{10}\text{N}_2\text{S}$: C, 69.00; H, 4.45; N, 12.38%. Found: C, 68.75; H, 4.45; N, 12.29%.

(Z)-2-(2-Pyrrol-2-ylethenyl)benzothiazole ((Z)-5). δ (ppm) 6.24 (d, $J = 12.0$ Hz, 1H, olefinic proton), 6.38 (m, 1H, pyrrole proton), 6.56 (m, 1H, pyrrole proton), 6.72 (d, $J = 12.0$ Hz, 1H, olefinic proton), 7.13 (m, 1H, pyrrole proton), 7.36 (td, 1H, $J = 7.3, 1.2$ Hz, benzothiazole proton), 7.51 (td, 1H, $J = 7.3, 1.2$ Hz, benzothiazole proton), 7.85 (dd, $J = 7.3, 1.2$ Hz, 1H, benzothiazole proton), 8.03 (dd, 1H, $J = 7.3, 1.2$ Hz, 1H, benzothiazole proton), 14.0 (br s, NH proton); mp = 80–81 °C.

In spectroscopy, Dotite Spectrosol or Luminasol were used as solvents without further purification.

Measurements

Absorption and fluorescence spectra were measured on a JASCO Ubest-55 and on a Hitachi F-4000 fluorescence spectrometer, respectively.

Laser flash photolyses were performed by using an excimer laser (Lambda Physik LPX-100, 308 nm, 20 ns fwhm) or excimer pumped dye laser (Lambda Physik LEXtra-100, 308 nm, 20 ns fwhm and Lambda Physik Scanmate, stilbene 3, 425 nm, 10 ns fwhm) as excitation light sources and a pulsed xenon arc (Ushio UXL-159) was used as a monitoring light source. A photomultiplier (Hamamatsu R-928) and a storage oscilloscope (Iwatsu TS-8123) were used for the detection.

Fluorescence lifetimes were determined with a picosecond laser system consisting of a titanium sapphire laser (Spectra Physics 3900 "Tsunami") operated with a CW Ar^+ laser (Spectra Physics 2060), a frequency doubler (SP-390), a pulse selector (SP-3980; ≈ 2 ps fwhm) and a streak scope (Hamamatsu C4334).

DSC measurements were performed with a Seiko DSC-220 and data module SSC-5500H.

Quantum yields of isomerization were determined with 366 nm light from a 400 W high-pressure mercury lamp through UV-35 and U-360 filters. The sample solution was deaerated with bubbling argon and irradiated for 5–15 min to keep the conversion to within 10%. Light intensity was determined by tris(oxalato)ferrate(III) actinometry.¹⁷ The concentration of each isomer was determined by high performance liquid chromatography through a column (Toso CN-80TS) eluting with ethyl acetate–*n*-hexane = 1 : 9.

Rate constants of acid-catalyzed thermal isomerization and equilibrium constants were determined by monitoring the absorbance of $(E)\text{-4}\cdot\text{H}^+$ in the presence of an appropriate amount of 0.1 M HCl (Wako analytical grade). The molar extinction coefficient of $(E)\text{-4}\cdot\text{H}^+$ was determined with the concentration of $[(E)\text{-4}] = 2.0 \times 10^{-5}$ M and $[\text{HCl}] = 1.2 \times 10^{-2}$ M.

Results and discussion

Absorption and fluorescence spectra

The absorption spectra of **4** and **5** were shown in Fig. 1. The

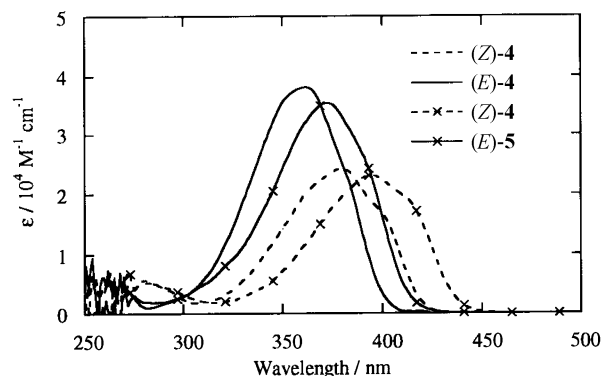


Fig. 1 Absorption spectra of **4** and **5** in benzene at room temperature.

molar extinction coefficient at the absorption maximum of $(Z)\text{-4}$ and $(Z)\text{-5}$ is smaller than that of $(E)\text{-4}$ and $(E)\text{-5}$. The absorption spectrum of $(Z)\text{-4}$ and $(Z)\text{-5}$ in benzene is shifted to the longer wavelength region compared with that of $(E)\text{-4}$ and $(E)\text{-5}$. Usually, the *cis* isomers exhibit absorption maxima at shorter wavelength compared with that of the *trans* isomers, since the aromatic ring and the C=C double bond take an almost planar conformation in the *trans* isomers, while the single bonds connecting the aromatic ring and the double bond are twisted to some extent due to the steric hindrance in the *cis* isomers. The absorption maximum of **5** appeared at longer wavelength than that of **4** by 15 nm and therefore, the singlet excitation energy of **5** is lower than that of **4**.

The unusual red shift of the absorption spectra in the *cis* isomers can be explained by the effect of intramolecular hydrogen bonding, which increases the conjugation in the *cis* isomers. In fact, in the ^1H NMR spectra, the signal of the NH proton of $(Z)\text{-4}$ and $(E)\text{-4}$ appeared at 14.0 ppm and 8.0 ppm, respectively in CDCl_3 . The considerable downfield shift of the NH proton signal in $(Z)\text{-4}$ indicates that $(Z)\text{-4}$ forms an $\text{NH} \cdots \text{N}$ intramolecular hydrogen bond in the ground state.

The difference in charge transfer character between $(Z)\text{-}$ and $(E)\text{-4}$ in the excited state may explain the above-mentioned observation that $(Z)\text{-4}$ exhibits absorption spectra at longer wavelength than $(E)\text{-4}$.

The absorption maximum (λ_{max}) of $(Z)\text{-4}$ does not linearly depend on the solvent polarity and is almost the same in all the solvents examined (Table 1). Thus, λ_{max} in methylcyclohexane and in DMSO appeared at 379 nm, while the value in acetonitrile (371 nm) and in methanol (373 nm) was at shorter wavelength. These results indicate that the presence of intramolecular hydrogen bonding in $(Z)\text{-4}$ in the above solvents.

The absorption maximum of $(E)\text{-4}$ shows a red shift with increasing solvent polarity from 356 nm in methylcyclohexane to 368 nm in DMSO. These results show that $(E)\text{-4}$ forms

Table 1 Molar extinction coefficient of λ_{max} of absorption spectra of **4** and **5**

Solvent	$\lambda_{\text{max}}/\text{nm}$ ($\epsilon/10^4 \text{ M}^{-1} \text{ cm}^{-1}$)			
	(E)-4	(Z)-4	(E)-5	(Z)-5
Methylcyclohexane	356 (4.1)	379 (2.9)	365 (4.4)	394 (2.7)
Benzene	362 (3.9)	380 (2.4)	373 (3.5)	394 (2.3)
Acetonitrile	356 (4.0)	371 (2.7)	369 (3.6)	386 (2.4)
Methanol	363 (4.4)	373 (2.9)	378 (3.4)	388 (2.2)
DMSO	368 (3.5)	379 (2.3)	388 (3.9)	393 (2.6)
Water	363	366		

intermolecular hydrogen bonds with methanol and DMSO, which may play some role on the behavior of **4** in the singlet excited state. In water, the absorption maximum of (*Z*)-**4** was still slightly red shifted than that of (*E*)-**4**. This result indicates that (*Z*)-**4** forms an intramolecular hydrogen bonding even in water.

The fluorescence spectra of **4** are shown in Fig. 2. At room

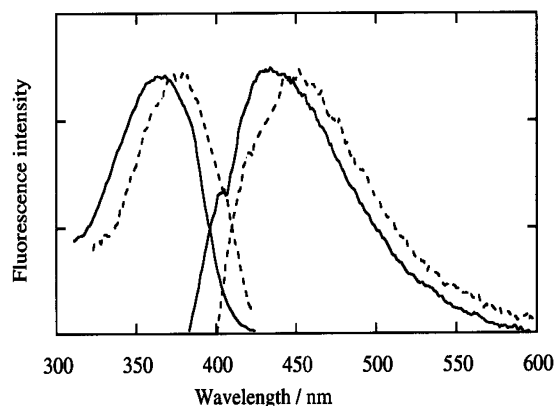


Fig. 2 Fluorescence and fluorescence excitation spectra of (*E*)-**4** (solid line) and (*Z*)-**4** (dashed line) in benzene at room temperature.

temperature, the quantum yield of fluorescence emission of **4** was determined to be 2×10^{-4} and 1×10^{-5} for (*E*)- and (*Z*)-**4**, respectively, while at 77 K, it was 0.5 for (*Z*)- and (*E*)-**4** in methylcyclohexane (Fig. 3). These results indicate that the

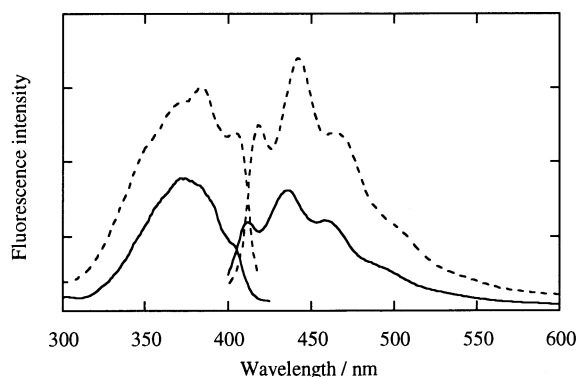


Fig. 3 Fluorescence and fluorescence excitation spectra of (*E*)-**4** (solid line) and (*Z*)-**4** (dashed line) in methylcyclohexane at 77 K.

excited singlet state of (*E*)- and (*Z*)-**4** should deactivate to the ground state by twisting around the double bond resulting in the *cis*-*trans* isomerization at room temperature, while at 77 K the fluorescence emission prevails over the isomerization due to the decrease of the rate constant of isomerization in the excited state. In addition, deactivation through the intramolecular hydrogen bonding in the *cis* isomer seems to be negligible compared with the other deactivation processes such as fluorescence emission. Therefore, intramolecular hydrogen bonding in the *cis* isomer should become weaker or be almost broken in the singlet excited state.

Fluorescence lifetimes of (*Z*)- and (*E*)-**4** were determined to be 2.3 ns and 1.6 ns, respectively, in methylcyclohexane and 2.0 ns and 1.9 ns in ethanol at 77 K. Similar fluorescence lifetimes were observed for (*Z*)- and (*E*)-**5** at 77 K: 3.2 ns and 1.5 ns in methylcyclohexane and 2.9 ns and 1.8 ns in ethanol. This also indicates that intramolecular hydrogen bonding would become weaker in the singlet excited state, and therefore could not participate in the deactivation pathways from the singlet excited state.

Differential scanning calorimetry (DSC) in **4**

The DSC experiments were performed at different, increasing temperatures ($2.5\text{--}7\text{ }^\circ\text{C min}^{-1}$). A typical example is shown in Fig. 4. Thus, the energy difference between (*Z*)- and (*E*)-**4** in the

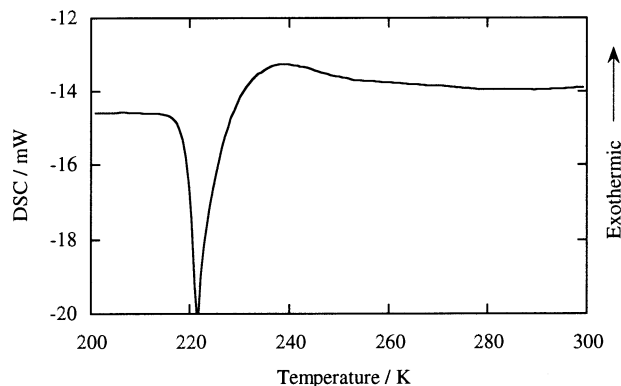


Fig. 4 DSC thermogram obtained for (*E*)-**4** increasing temperature ($7\text{ }^\circ\text{C min}^{-1}$).

ground state was determined to be 5 kcal mol^{-1} . The value obtained indicates that (*Z*)-**4** is more stable than (*E*)-**4** by 5 kcal mol^{-1} , probably due to the presence of intramolecular hydrogen bonding in (*Z*)-**4**. In addition, the activation energy of *trans*-to-*cis* isomerization was calculated to be 33 kcal mol^{-1} by similar treatment to that reported by Kissinger.¹⁸

Quantum yield of isomerization and the photostationary state isomer ratio

The quantum yield of *trans*-*cis* isomerization (Φ_{t-c}) of **4** was determined to be 0.64 and 0.54 in benzene and methanol, respectively, and is slightly higher than that of *cis*-*trans* isomerization (Φ_{c-t}), which is 0.41 and 0.48 in benzene and in methanol, respectively. The quantum yield of isomerization for **5** was determined to be similar to that of **4**. The photostationary state *cis*-to-*trans* isomer ratio ($[c]/[t]_{\text{pss}}$) of **4** was determined to be 71 : 29 and 65 : 35 in benzene and in methanol, respectively. The ($[c]/[t]_{\text{pss}}$) values for **5** were determined to be 81 : 19 and 76 : 24 in benzene and in methanol, respectively. The observed ($[c]/[t]_{\text{pss}}$) values are quite similar to those calculated by the combination of the molar extinction coefficient of the *cis* (ϵ_c) and *trans* isomers (ϵ_t) at the excitation wavelength and the quantum yield of isomerization ($[c]/[t]_{\text{pss}} = (\epsilon_t/\epsilon_c) \times (\Phi_{t-c}/\Phi_{c-t})$). These values, together with the values determined in acetonitrile are summarized in Table 2. The Φ_{c-t} value is higher, but Φ_{t-c} is lower in polar protic solvents than in less polar solvents. The distortion of the conical intersection may explain the above solvent effect.

Triplet sensitized isomerization was effected by biacetyl or Michler's ketone as triplet sensitizers with irradiation at 436 nm or 313 nm from a high pressure mercury lamp. On triplet sensitization, both *cis*-to-*trans* and *trans*-to-*cis* isomeriz-

Table 2 Quantum yield of isomerization and photostationary state isomer ratio of **4** and **5** determined on irradiation at 366 nm at room temperature

	Solvent	Φ_{t-c}	Φ_{c-t}	$[c]/[t]_{\text{pss}}$	
				Found	Calcd.
4	Methylcyclohexane			71 : 29	
	Benzene	0.64	0.41	71 : 29	73 : 27
	Methanol	0.54	0.48	65 : 35	63 : 37
	Acetonitrile			70 : 30	
5	Benzene	0.71	0.37	81 : 19	83 : 17
	Methanol	0.64	0.44	76 : 24	73 : 27
	Acetonitrile	0.72	0.40	71 : 29	77 : 23

ation occurred to give the isomer ratio at the photostationary state of $([c]/[t])_{\text{pss}} = 40/60$.

Effect of HCl on the behavior of 4

The absorption spectra of (*E*)-4 in acetonitrile in the presence of HCl_{aq} appeared in the longer wavelength region with a maximum at 430 nm compared with the absorption maximum of 356 nm in pure acetonitrile as shown in Fig. 5. The concen-

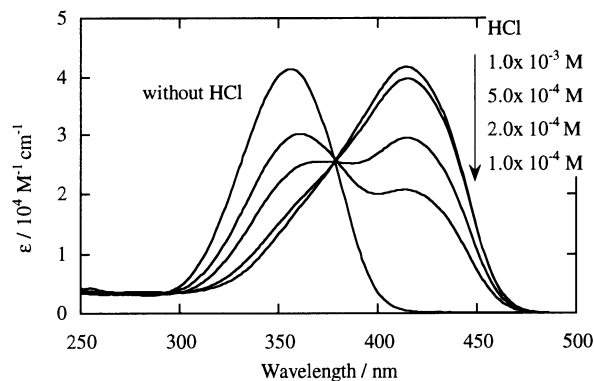


Fig. 5 Absorption spectra of (*E*)-4 in the presence of HCl in acetonitrile.

tration of HCl was changed from 1×10^{-4} M to 1×10^{-3} M by addition of 1 M HCl solution. Thus, the absorbance at 356 nm decreased with the increase of HCl_{aq} with a concomitant increase of the absorbance at 430 nm. The isosbestic point appeared at 375 nm and finally, in the presence of 1×10^{-3} M of HCl_{aq} , the absorption spectrum can be assigned to that of the protonated form. In contrast, the absorption spectrum of (*Z*)-4 observed just after the addition of HCl_{aq} was identical with that in the absence of HCl_{aq} in acetonitrile. The absorption spectra of (*Z*)-4 in the presence of HCl_{aq} in acetonitrile gradually changed and the absorption maximum shifted from 371 nm to 420 nm over a period of 240 min at 299 K (Fig. 6).

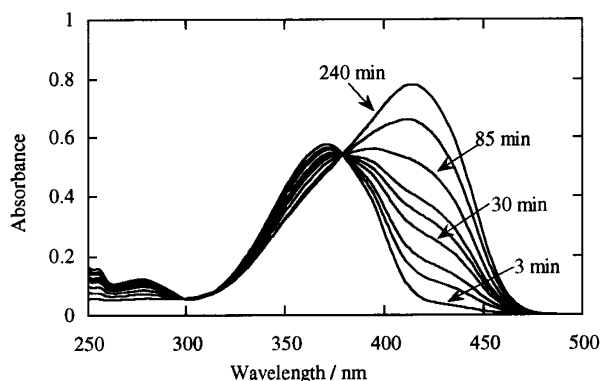
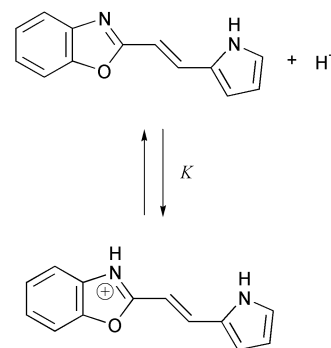


Fig. 6 Change of the absorption spectrum of (*Z*)-4 (2.0×10^{-5} M) in the presence of HCl (1.0×10^{-3} M) at 299 K.

The ^1H NMR spectra of 4 were measured in methanol- d_4 in the presence of HCl_{aq} . The ^1H NMR spectrum of (*Z*)-4 in methanol- d_4 did not shift after the addition of 1 drop of 12 M HCl, while the peaks in ^1H NMR spectrum of (*E*)-4 shifted upon addition of HCl. For example, the peaks of the olefinic proton of (*E*)-4 shifted from 6.68 and 7.68 ppm to 6.84 and 8.14 ppm, suggesting that protonation took place at the nitrogen atom of benzoxazole ring to give (*E*)-4 $\cdot\text{H}^+$.

As shown in Fig. 6, the absorption spectrum observed at 240 min after the addition of HCl_{aq} is the same as that of (*E*)-4 in the presence of HCl_{aq} . These results clearly show that the thermal *cis*-to-*trans* isomerization of 4 (2.0×10^{-5} M) occurred in the presence of HCl_{aq} (2×10^{-3} M). The rate constant of *cis*-to-*trans* isomerization (k_{c-t}) was determined to be 4×10^{-8} s $^{-1}$ at



298 K. The k_{c-t} value increased with increasing temperature (Fig. 7). Thus, the temperature effect on the k_{c-t} value gave the

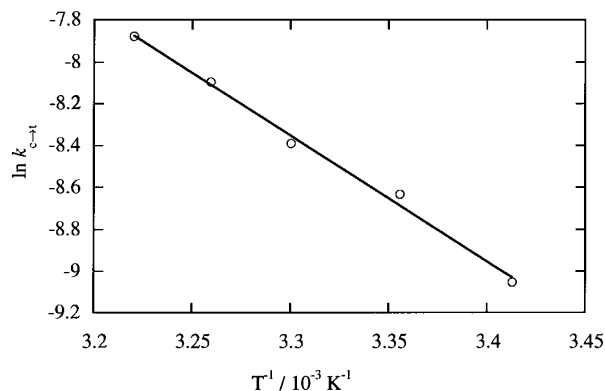


Fig. 7 Arrhenius plot for the *cis*-to-*trans* thermal isomerization of (*Z*)-4 (2.0×10^{-5} M) in the presence of HCl (1.0×10^{-3} M).

activation energy (E_a) and preexponential factor (A) of the Arrhenius parameter for (*Z*)-4 $\cdot\text{H}^+$ \rightarrow (*E*)-4 $\cdot\text{H}^+$ to be 11.9 kcal mol $^{-1}$ and 9.6×10^4 s $^{-1}$, respectively.

Upon irradiation at 366 nm, 4 (2.0×10^{-5} M) underwent *trans*-*cis* isomerization in the presence of HCl_{aq} ($[\text{HCl}] = 2 \times 10^{-3}$ M) to give the isomer mixture at the photostationary state ($([c]/[t])_{\text{pss}} = 41/59$). The addition of HCl_{aq} to 4 in acetonitrile did not significantly affect the photoisomerization behavior, as indicated from the ratio of the quantum yield of isomerization estimated from the ratio of molar extinction coefficient of (*Z*)- and (*E*)-4 at 366 nm ($\Phi_{t-c}/\Phi_{c-t} = ([c]/[t])_{\text{pss}} \times (\epsilon_z/\epsilon_t) = (41/59) \times (2.6 \times 10^4/2.0 \times 10^4) = (0.48/0.52)$). However, as mentioned above the *cis* isomer produced underwent isomerization to the *trans* isomer even in the ground state, when the HCl_{aq} was present.

The temperature effect on the absorption spectra of (*E*)-4 ($([E]-4] = 2.0 \times 10^{-5}$ M) in the presence of HCl_{aq} ($[\text{HCl}] = 2 \times 10^{-4}$ M) is shown in Fig. 8. Since the absorbance at 356 nm (non-protonated form) increased with the increase of the tem-

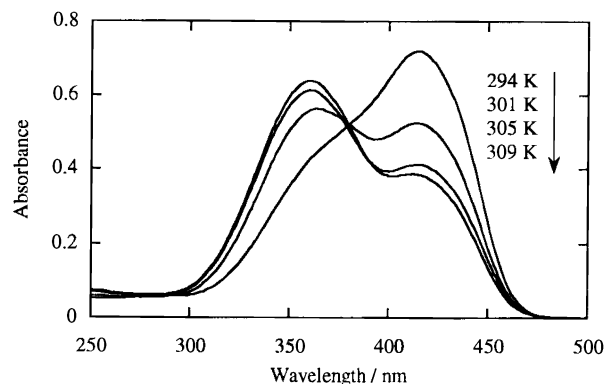


Fig. 8 Effect of temperature on the absorption spectrum of (*E*)-4 (2.0×10^{-5} M) in the presence of HCl (2.0×10^{-4} M) in acetonitrile.

perature with concomitant decrease of the absorbance at 430 nm (protonated form), the protonated form favors low temperature. Thus, the equilibrium constant (K) was estimated to be $8.2 \times 10^3 \text{ M}^{-1}$ (at 298 K), $7.2 \times 10^3 \text{ M}^{-1}$ (at 299 K), $5.4 \times 10^3 \text{ M}^{-1}$ (at 301 K), and $3.1 \times 10^3 \text{ M}^{-1}$ (at 305 K). From these experiments the enthalpy difference ΔH between the neutral (E)-**4** and the protonated (E)-**4**· H^+ can be estimated to be $25.5 \text{ kcal mol}^{-1}$ by using the van't Hoff plot for the temperature effect on the absorption spectra shown in Fig. 9.

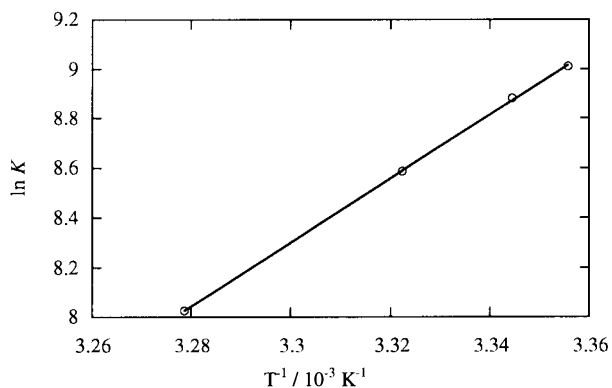


Fig. 9 The van't Hoff plot for the equilibrium between (E)-**4** ($2 \times 10^{-5} \text{ M}$) and (E)-**4**· H^+ in the presence of HCl ($2.0 \times 10^{-4} \text{ M}$) in acetonitrile.

Under the same acidic conditions, the fluorescence spectrum of (E)-**4** was observed in the longer wavelength region with the emission maximum at 480 nm, which is very much shifted to the longer wavelength compared with that of (E)-**4** in pure acetonitrile as shown in Fig. 10. The entropy difference for the

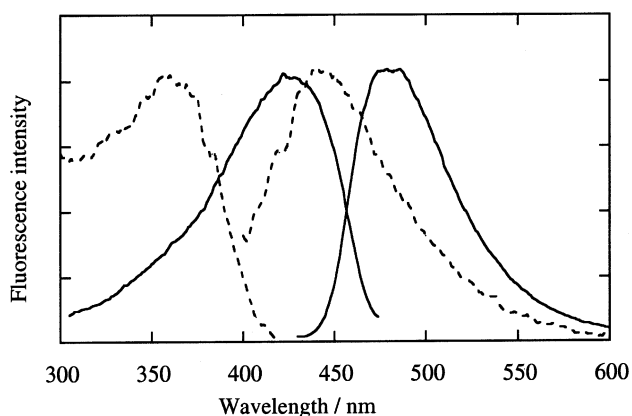


Fig. 10 Fluorescence and fluorescence excitation spectra of (E)-**4** in the absence of HCl (dashed line) and in the presence of HCl ($1.2 \times 10^{-2} \text{ M}$) in acetonitrile.

protonation in the ground state was estimated to be the same as that in the excited singlet state. Therefore, the $\text{p}K_{\text{a}}$ values can be estimated from the Förster cycle¹⁹ to be 3.9 in the ground state and 10.6 in the singlet excited state, respectively at 295 K. These results suggest that the acidity of the benzoxazole ring in the excited singlet state is lower than that in the ground state.

Laser flash photolysis

On direct irradiation of **4** and **5** at 308 nm or 425 nm, transient species were not observed.

On triplet sensitization with benzophenone excited by a 308 nm excimer laser or with biacetyl excited by a 425 nm dye laser, (Z)- and (E)-**4** gave transient absorption spectra with $\lambda_{\text{max}} = 450 \text{ nm}$ as shown in Fig. 11. Decay profiles monitored at 450–800 nm were fitted to a single exponential analysis and the rate constant was determined to be $1.0 \times 10^6 \text{ s}^{-1}$ under argon.

These transients were quenched by oxygen with a rate con-

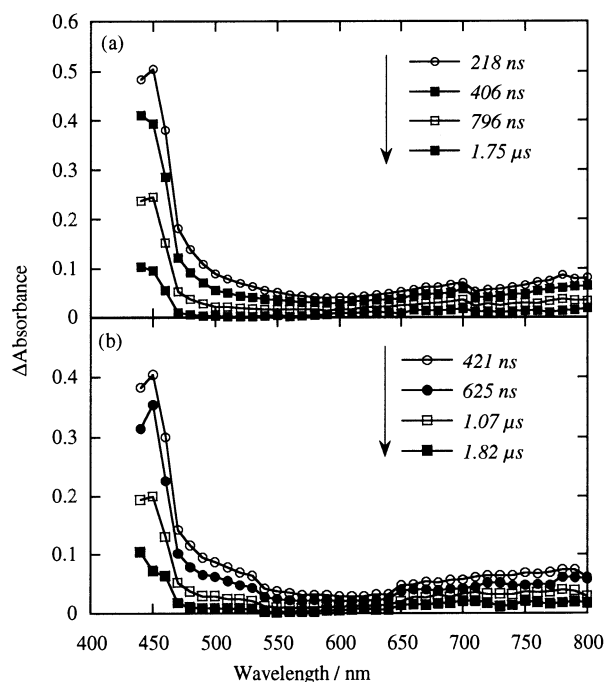


Fig. 11 Transient absorption spectra of (E)-**4** (a) and (Z)-**4** (b) observed on biacetyl sensitization. $[\mathbf{4}] = 2 \times 10^{-3} \text{ M}$, $[\text{biacetyl}] = 0.07 \text{ M}$ in benzene. The excitation wavelength was 425 nm.

stant of $4.4 \times 10^9 \text{ M}^{-1} \text{ s}^{-1}$. Based on the observation of the triplet state with considerably long lifetime and the observed quenching rate constant by oxygen being nearly $\frac{1}{5}$ of the diffusion controlled quenching rate constant [$(2-3) \times 10^{10} \text{ M}^{-1} \text{ s}^{-1}$], the observed transient can be assigned to the *trans* triplet state.

On benzil sensitization, the triplet energy of (Z)- and (E)-**4** was estimated by determining the quenching rate constant of the benzil triplet ($E_{\text{T}} = 53.4 \text{ kcal mol}^{-1}$)¹⁷ by (Z)- or (E)-**4**. The quenching rate constants (k_{q}) were determined to be $(1.5 \pm 0.1) \times 10^9$ and $(2.4 \pm 0.1) \times 10^9 \text{ M}^{-1} \text{ s}^{-1}$ for (Z)- and (E)-**4**, respectively. These values are smaller than the diffusion-controlled rate constant $6.3 \times 10^9 \text{ s}^{-1}$.²⁰ Therefore, the energy transfer process should be endothermic and the triplet energy of **4** can be estimated by means of eqn. (1)²¹ to be 54.1 and 53.7 kcal mol^{-1} for *cis*- and *trans*-isomers, respectively.

$$k_{\text{q}} = k_{\text{diff}} \exp(-\Delta E_{\text{a}}/RT) / [1 + \exp(-\Delta E_{\text{a}}/RT)] \quad (1)$$

Potential energy surface of *cis*-*trans* isomerization of **4**

In aprotic solvents such as benzene, the stabilization energy of (Z)-**4** due to the intramolecular hydrogen bonding was estimated to be 5 kcal mol^{-1} and the activation energy of *trans*-to-*cis* isomerization in the ground state was estimated to be 33 kcal mol^{-1} by DSC experiments. The singlet excitation energies of *cis*- and *trans*-**4** were found to be $69.4 \text{ kcal mol}^{-1}$ and $72.4 \text{ kcal mol}^{-1}$, respectively, from their absorption and fluorescence spectra. Based on these results, the potential energy surface of isomerization of **4** in benzene was depicted as shown in Fig. 12.

At room temperature, the quantum yield of fluorescence emission was determined to be 4×10^{-4} and 4×10^{-5} for (E)-**4** and (Z)-**4**, respectively. In addition, no transient absorption spectrum was observed upon laser flash photolysis. Furthermore, the sum of quantum yields of isomerization ($\Phi_{\text{i-c}} + \Phi_{\text{c-i}}$) for **4** and **5** in all the solvents examined is nearly 1. These results indicate that both (Z)-**4** and (E)-**5** underwent *cis*-*trans* isomerization exclusively from the excited singlet state.

Although (Z)-**4** forms intramolecular hydrogen bonds, the lifetime of the fluorescence emission of (Z)-**4** was similar to that of (E)-**4** in methylcyclohexane and ethanol at 77 K. This also indicates that the intramolecular hydrogen bonding would

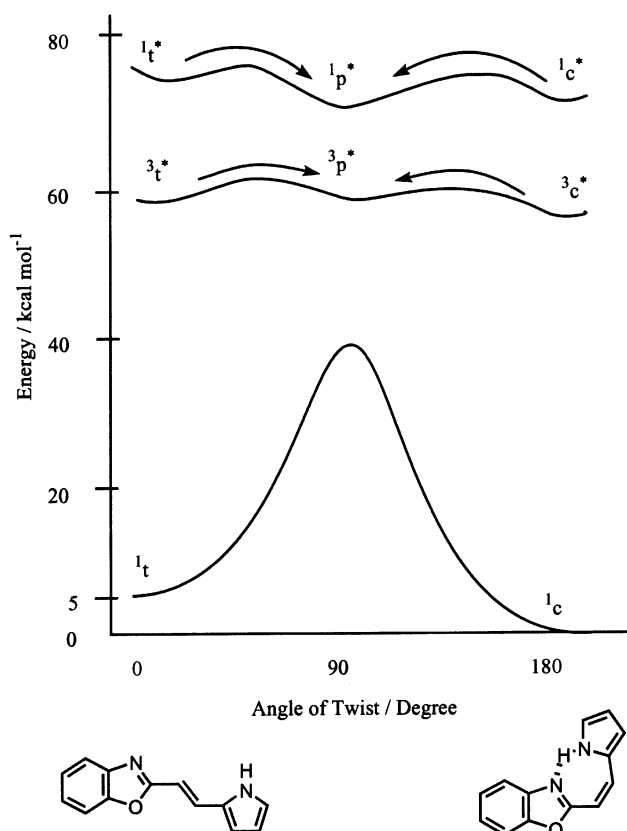


Fig. 12 Potential energy surface of isomerization of **4** in benzene.

become weaker in the excited singlet state, and therefore the intramolecular hydrogen bonding could not participate in the deactivation pathways from the singlet excited state.

Both (*Z*)-**4** and (*E*)-**4** gave the same T–T absorption spectra with the same decay constants on triplet sensitization. From the triplet lifetime and the photostationary state isomer composition determined on triplet sensitization, it was found that the equilibration between the *trans*-form and the perpendicular form was established in the excited triplet state. The rate constant of the deactivation from the perpendicular ($^3p^*$) (k_{pd}) and the *trans* triplet state ($^3t^*$) (k_{td}) could be estimated to be $2 \times 10^7 \text{ s}^{-1}$ and $2 \times 10^4 \text{ s}^{-1}$, respectively.²² Thus, the equilibrium constant, K_{tp} , between $^3t^*$ and $^3p^*$ ($[^3p^*]/[^3t^*]$) is estimated to be *ca.* 0.05 from the observed triplet lifetime by using eqn. (2), where $^3t^*$ is much more stable than $^3p^*$.

$$\tau_T = (1 + K_{tp}) / (K_{tp}k_{pd} + k_{td}) \quad (2)$$

Photochromic properties

At the photostationary state, the proportion of the *cis*-isomers of **4** and **5** was higher in benzene than in methanol. In addition, *cis*-isomers exhibited a yellow absorption maximum at longer wavelength compared to the *trans*-isomers. Therefore, with the aid of intramolecular hydrogen bonding one can extend the absorption spectra of the molecule to the longer wavelength region as observed in the intramolecularly hydrogen bonded compounds (*Z*)-**4** and (*Z*)-**5**, and can construct photochromic materials by choosing appropriate excitation wavelengths. Furthermore, the addition of acid changed the color of the solution and the photochromic behavior, where *cis* isomers are

less stable in the ground state and gradually revert to the *trans* isomers within several tens to hundreds of minutes. Thus, by photoirradiation one can produce the *cis* isomers of **4** and **5**, while without light only *cis*-to-*trans* isomerization was observed and one can obtain the solution of only the *trans* isomers in the dark in the presence of acid.

Conclusions

Compounds **4** and **5** form intramolecular hydrogen bonds in the *cis*-form, and therefore, the absorption spectra of *cis* isomers are shifted to longer wavelength compared with the *trans* isomers. In the singlet excited state as well as in the triplet state the intramolecular hydrogen bonding in (*Z*)-**4** and (*Z*)-**5** seems to be broken and therefore, *cis*–*trans* isomerization in **4** and **5** occurs efficiently. The *cis*-to-*trans* ratio at the photostationary state ($[c]/[t]_{\text{pss}}$) was 2.4 and 4.3 for **4** and **5**, respectively, in benzene, and decreased in polar protic solvents. The sum of the quantum yields of isomerization was almost 1. Therefore, **4** and **5** mainly undergo *cis*–*trans* isomerization in the excited state without undergoing hydrogen atom transfer to give the tautomer in the excited state.

Acknowledgements

This work was supported by a Grant-in-Aid for Scientific Research (No. 10440166) from the Ministry of Education, Science, Sports and Culture, Japan, and by the Research Foundation for Opto-Science and Technology.

References

- J. S. Stephan and K. H. Grellmann, *J. Phys. Chem.*, 1995, **99**, 10066.
- W. Al-Soufi, K. H. Grellmann and B. Nickel, *Chem. Phys. Lett.*, 1990, **174**, 609.
- P. T. Chou, W. C. Cooper, J. H. Clements, S. L. Studer and C. P. Chang, *Chem. Phys. Lett.*, 1993, **216**, 300.
- P. T. Chou, M. L. Martinez and S. L. Studer, *Chem. Phys. Lett.*, 1992, **195**, 586.
- S. Nagaoka, A. Itoh, K. Mukai and U. Nagashima, *J. Phys. Chem.*, 1993, **97**, 11385.
- M. Itoh and Y. Fujiwara, *J. Am. Chem. Soc.*, 1985, **107**, 1561.
- G. Yang, F. Morelet-Savary, Z. Peng, S. Wu and J.-P. Fouassier, *Chem. Phys. Lett.*, 1996, **256**, 536.
- M. Ikegami and T. Arai, *Chem. Lett.*, 2000, 996.
- F. D. Lewis, B. A. Yoon, T. Arai, T. Iwasaki and K. Tokumaru, *J. Am. Chem. Soc.*, 1994, **116**, 3171.
- T. Arai, M. Obi, T. Iwasaki, K. Tokumaru and F. D. Lewis, *J. Photochem. Photobiol. A: Chem.*, 1995, **96**, 65.
- T. Arai, M. Moriyama and K. Tokumaru, *J. Am. Chem. Soc.*, 1994, **116**, 3171.
- M. Obi, H. Sakuragi and T. Arai, *Chem. Lett.*, 1998, 169.
- T. Arai and Y. Hozumi, *Chem. Lett.*, 1998, 1153.
- Y. Yang and T. Arai, *Tetrahedron Lett.*, 1998, **39**, 2617.
- T. Arai and M. Ikegami, *Chem. Lett.*, 1999, 965.
- E. C. Taylor and S. F. Martin, *J. Am. Chem. Soc.*, 1974, **96**, 8095.
- Handbook of Photochemistry*, eds. S. L. Murov, I. Carmichael and G. L. Hug, Marcel Dekker, New York, 1993.
- H. E. Kissinger, *Anal. Chem.*, 1957, **29**, 1702.
- Th. Förster, *Z. Electrochem.*, 1950, **54**, 42.
- The diffusion-controlled quenching rate constant was determined by Stern–Volmer analysis for the triplet quenching of benzophenone triplet ($E_T = 69 \text{ kcal mol}^{-1}$)¹⁷ by naphthalene ($E_T = 60 \text{ kcal mol}^{-1}$)¹⁷ to be $6.3 \times 10^9 \text{ M}^{-1} \text{ s}^{-1}$ in benzene at 295 K.
- K. Sandros, *Acta. Chem. Scand.*, 1964, **18**, 2355.
- T. Arai and K. Tokumaru, *Chem. Rev.*, 1993, **93**, 23.